ARTICLE

Influence of the early-life gut microbiota on the immune responses to an inhaled allergen

Timothy C. Borbet[1], Miranda B. Pawline[1], Xiaozhou Zhang[2], Matthew F. Wipperman[3,4], Sebastian Reuter[5], Timothy Maher[1], Jackie Li[1], Tadasu Iizumi[1,6], Zhan Gao[6], Megan Daniele[1,7], Christian Taube[5], Sergei B. Koralov[1], Anne Müller[2]✉ and Martin J. Blaser[6]✉

Antibiotics, among the most used medications in children, affect gut microbiome communities and metabolic functions. These changes in microbiota structure can impact host immunity. We hypothesized that early-life microbiome alterations would lead to increased susceptibility to allergy and asthma. To test this, mouse pups between postnatal days 5–9 were orally exposed to water (control) or to therapeutic doses of azithromycin or amoxicillin. Later in life, these mice were sensitized and challenged with a model allergen, house dust mite (HDM), or saline. Mice with early-life azithromycin exposure that were challenged with HDM had increased IgE and IL-13 production by $CD4^+$ T cells compared to unexposed mice; early-life amoxicillin exposure led to fewer abnormalities. To test that the microbiota contained the immunological cues to alter IgE and cytokine production after HDM challenge, germ-free mice were gavaged with fecal samples of the antibiotic-perturbed microbiota. Gavage of adult germ-free mice did not result in altered HDM responses, however, their offspring, which acquired the antibiotic-perturbed microbiota at birth showed elevated IgE levels and $CD4^+$ cytokines in response to HDM, and altered airway reactivity. These studies indicate that early-life microbiota composition can heighten allergen-driven Th2/Th17 immune pathways and airway responses in an age-dependent manner.

Mucosal Immunology (2022) 15:1000–1011; https://doi.org/10.1038/s41385-022-00544-5

INTRODUCTION

Global asthma incidence has increased over the past five decades, with 300 million people currently affected[1]. Asthma is clinically diverse and categorized into different endotypes. The type 2 (T2) high endotype has increased type 2 cytokine responses, characterized by production of Interleukin (IL)-4, IL-5 and IL-13 by either T helper 2 (Th2) cells or type 2 innate lymphocytes. Asthmatic children without these T2 signatures are classified as the T2-low endotype[2,3]. T2-high asthma, including early-onset allergic, late-onset eosinophilic, and exercise-induced asthma, mostly responds to medications targeting T2 immune responses[2–4]. The T2-low endotype includes neutrophilic and obesity-related forms of asthma, which are characterized by type 17 immune responses and neutrophil recruitment that mediate pulmonary inflammation, and have fewer available therapies[2,5]

Early-life antibiotic use has been associated with increased asthma risk in epidemiological studies[6–9], and reducing community-wide antibiotic exposure has been associated with diminished asthma incidence[10]. Asthma is part of an allergic continuum also including atopic dermatitis, food allergy, and allergic rhinitis; early-life antibiotic exposure has been associated with increased risk of all of these disorders[11–15]. These observations support the hypothesis that early-life antibiotic use is causally involved in asthma predisposition, but direct evidence has been lacking.

Amoxicillin and azithromycin are the two most commonly prescribed pediatric antibiotics in the U.S. and globally[6,16,17]. The developing early-life microbiota is perturbed by antibiotics, with effects related to antibiotic class, dose, duration, and host age during exposure[18–20]. Early-life microbiome perturbation can change microbial metabolites and alter microbiome resilience and colonization resistance, altering host immune and metabolic development[21–26].

We now report studies of early-life administration of azithromycin and amoxicillin to mice, at levels prescribed in children, that highlight interactions of microbiome perturbation with host age, and downstream inflammatory and immune consequences. We provide direct evidence that azithromycin perturbation of the early-life microbiota enhances the immunological and physiological features of allergen-driven responses.

RESULTS

Early-life antibiotic exposures alter responses to allergen challenge

To assess whether a clinically relevant antibiotic exposure alters susceptibility to allergic airway inflammation, C57BL/6

[1]Department of Pathology, New York University School of Medicine, New York, NY, USA. [2]Institute of Molecular Cancer Research, University of Zurich, Zurich, Switzerland. [3]Immunology Program, Sloan Kettering Institute, New York, NY, USA. [4]Clinical and Translational Science Center, Weill Cornell Medicine, New York, NY, USA. [5]Department of Pulmonary Medicine, Experimental Pneumology, University Hospital Essen—Ruhrlandklinik, Essen, Germany. [6]Center for Advanced Biotechnology and Medicine, Rutgers University, New Brunswick, NJ, USA. [7]Department of Pediatrics, New York-Presbyterian Morgan Stanley Children's Hospital Columbia Irving Medical Center, New York, NY, USA. ✉email: mueller@imcr.uzh.ch; martin.blaser@cabm.rutgers.edu

Received: 18 January 2021 Revised: 4 June 2022 Accepted: 15 June 2022
Published online: 16 July 2022

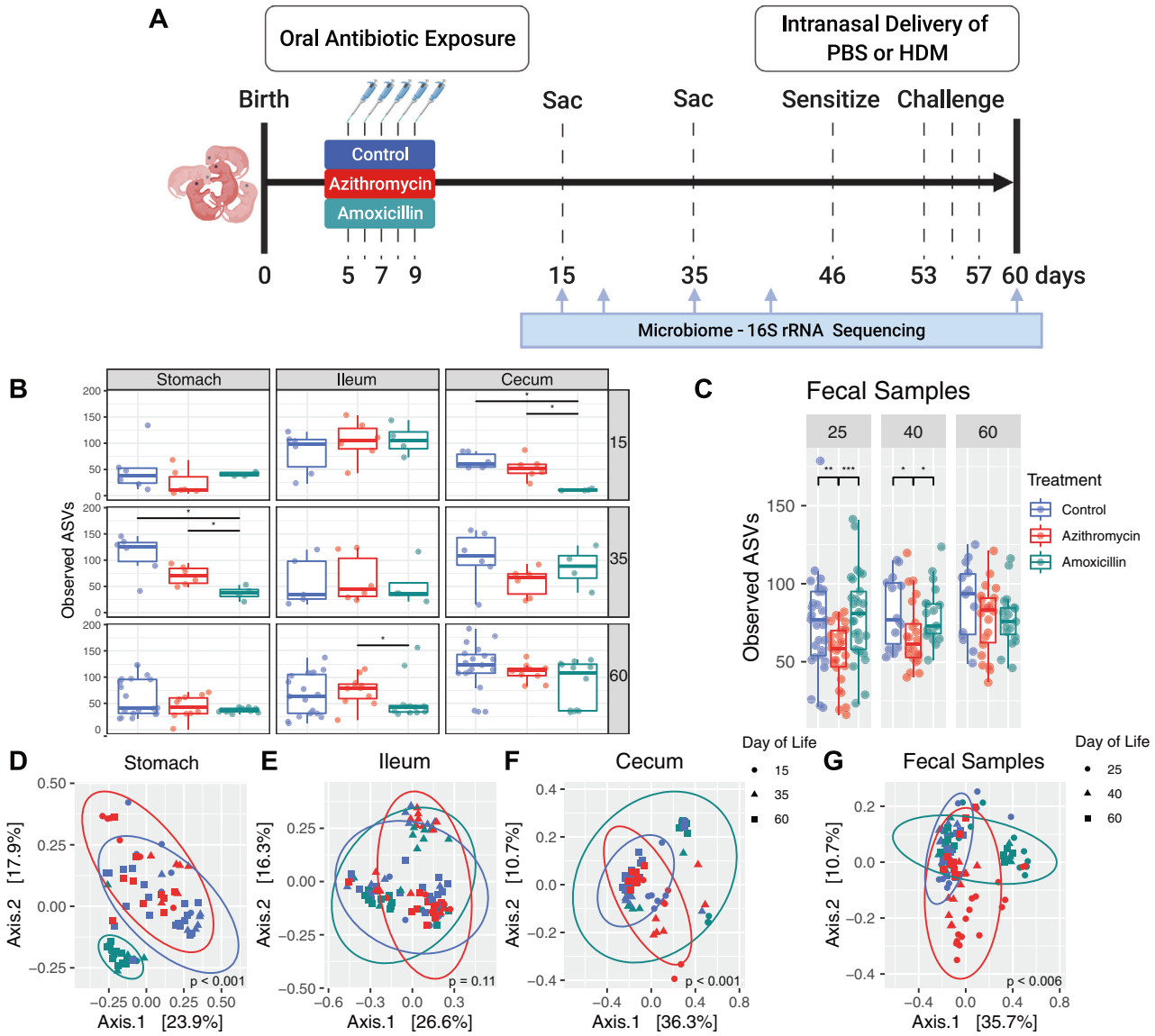

Fig. 1 Evaluation of microbiota composition in antibiotic-exposed mice. a Mice received early-life treatment with azithromycin, amoxicillin, or not—control, between P5-9 by direct oral administration; dams were unexposed. For each independent experiment, there were at least 2 or 3 litters per treatment group. At P46, mice were intranasally sensitized with 1 µg of HDM antigen or PBS as a negative control for HDM sensitization. One week later, mice received three separate intranasal challenges with 10 µg of HDM antigen, or again with PBS as a negative control. All mice were sacrificed 3 days after the last challenge at P60. DNA extracted from mouse stomach tissue, ileal tissue with contents, colon tissue with contents and fecal pellets and was subjected to 16S rRNA sequencing. Tissue samples were collected at sacrifice on days 15, 35 and 60, while fecal samples were collected on days 25, 40, and 60. Analysis of alpha diversity (observed ASVs) (**b**, **c**) and beta diversity (**d**–**g**) (unweighted UniFrac) are from one representative experiment. Significance for alpha diversity was determined by a nonparametric one-way ANOVA (*$p < 0.05$; **$p < 0.01$; ***$p < 0.001$) and for beta diversity, a permutational multivariate analysis of variance was performed to compare antibiotic exposure, day of life, and the interaction of both factors (a p value for each comparison is reported on the UniFrac plot). Results are shown for: **d** stomach (18.8% variance explained by treatment, 7.2% by day of life, and 9.3% by both); **e** ileum (4.9% variance explained by treatment, 7.7% by day of life, and 6.8% by both); **f** cecum (9.8% variance explained by treatment, 17.9% by day of life, and 6.3% by both); and **g** fecal pellets (13.4% variance explained by treatment, 7.4% by day of life, and 9.3% by both).

select-pathogen-free (SPF) pups were orally dosed from postnatal day (P)5 for 5 days with azithromycin or amoxicillin at pharmacological levels for children (amoxicillin, 100 mg/kg of bodyweight/day; azithromycin, 30 mg/kg of bodyweight/day) or water as a control (Fig. 1a). Following antibiotic exposure, on P46, mice were sensitized intranasally with HDM extract, or PBS as a negative control, and subsequently challenged intranasally three times with HDM or PBS. Mice were euthanized at P60 and immune responses to HDM were compared across the groups, 50 days after the antibiotic exposure had ended. We first asked whether the antibiotic exposures affected inflammatory responses to HDM antigen. Analysis of bronchoalveolar lavage (BAL), collected to assess leukocytic airway infiltration, indicated that mice exposed to azithromycin or amoxicillin during early-life, and subsequently sensitized and challenged with HDM, compared to HDM-sensitized and -challenged control mice, led to no significant changes in BAL cellularity (Fig. S1A–C). However, azithromycin-HDM mice had increased serum (Fig. S1D) and lung (Fig. S1E) total IgE levels, which were strongly correlated (Fig. S1F). In the PBS-challenged mice, prior antibiotic exposure did not affect BAL

cellularity, eosinophilia, or IgE levels (Fig. S1A–F). In total, these results indicate that early-life antibiotic exposures to azithromycin led to increased IgE responses following antigen challenge.

We then asked whether differences in Th2 or Th17 cytokines would explain the IgE patterns observed in mice that had early-life antibiotic exposure. First, compared to unexposed mice, azithromycin-exposed mice had an increase in lung $CD4^+$ T cell infiltration when sensitized and challenged with HDM (Fig. S1H). Among the mice that were HDM-sensitized/challenged, those exposed to azithromycin had higher pulmonary IL-13 production at P60 than the unexposed controls (Fig. S1G, I), consistent with higher IgE titers (Fig. S1D, E). Mice that had been exposed to amoxicillin and were then subsequently challenged with HDM had a higher frequency of IL-17A-producing $CD4^+$ Th cells than untreated controls (Fig. S1J). There were no significant differences in IFNγ production in any experimental group (Fig. S1K). We next sought to determine if these cytokine changes in antibiotic-exposed mice affected lung inflammation. Histological examination of lungs showed increased inflammatory scores and PAS+ cells related to the HDM challenge, but no significant differences with respect to prior antibiotic exposure (Fig. S2A–E). As there were no differences in lung inflammation (Fig. S2A–C), we did not expect any deficits in $FoxP3^+$ regulatory T cells (Tregs) and peripherally induced (p)Treg populations in the lung tissue in response to antibiotic exposure, and this was indeed the case (Fig. S2F). In total, these findings indicate that the early-life immunological perturbations were mostly associated with azithromycin exposure, and limited to heighted IgE responses, and increased lung $CD4^+$ T cell infiltration and IL-13 production.

Role of the microbiota in altering immunological responses

We then sought to determine if the differences observed in the antibiotic-exposed mice were due to direct effects of the drugs on the murine immune system, or whether they were transduced via perturbation of the microbiome. To address this, germ-free pups were treated with antibiotics, or not, and later sensitized and challenged with HDM, exactly as outlined in Fig. 1a. At P60, no differences in BAL cellularity or granulocyte frequency were found between the antibiotic-exposed or unexposed germ-free mice (Fig. S3A). Flow cytometric analysis of lung tissue also showed no significant differences in lung $CD4^+$ T cell abundance or frequencies with respect to antibiotic exposure (Fig. S3B). As observed in the SPF mice (Fig. S1B, G–J), the proportions of eosinophils and Th cells rose in mice challenged with HDM compared with PBS, but there were no significant differences in relation to the antibiotic exposure (Fig. S3A–C). Thus, in the absence of a microbiota, antibiotic treatment had no discernable impact on immune responses to allergen challenge. These results provide evidence that the observed antibiotic-driven effects on the immune responses to HDM are microbiota-dependent and do not result from the direct drug interactions with murine tissues, consistent with prior results[19].

Identification of taxa perturbed by the early-life antibiotic exposures

To determine whether antibiotic-exposure led to microbial differences in the experimental mice, we examined gastrointestinal and pulmonary samples using 16S rRNA sequencing. Antibiotic exposure led to significantly reduced representation of amplicon sequence variants (ASVs) in the gastric microbiota at P35 (Fig. 1b). The fecal microbiota of azithromycin-exposed mice showed significantly reduced ASVs at P25 and P40 (Fig. 1c). These findings indicate a reduction in taxon richness for at least a month following the antibiotic exposure with partial recovery, later in life (Fig. 1c). Utilizing unweighted UniFrac analysis across multiple timepoints (Fig. 1d–g) and plots of taxonomic abundance at P60 (Fig. S4), amoxicillin, but not azithromycin, altered gastric microbiota composition consistently at all timepoints (Fig. 1d and Fig. S4A). There were no differences in the ileal microbiota (Fig. 1e and Fig. S4B), the cecal microbiota was altered by exposure to either antibiotic across all timepoints (Fig. 1f and Fig. S4C). Both antibiotic regimens changed colonic community structure, determined by analysis of serially obtained fecal samples (Fig. 1g and Fig. S4D).

Each of the antibiotic exposures led to significantly altered colonic representation of multiple ASVs, with unsupervised hierarchical clustering of differentially abundant ASVs showing that colonic samples from azithromycin-exposed mice were distinct from the other treatment groups (Fig. 2). By P60, control mice had high abundances of Bacteroidota (especially Muribaculaceae species), which did not occur in mice with early-life antibiotic exposure. To assess changes in Muribaculaceae, the abundance of all Muribaculaceae strains, at the genus level, was evaluated in fecal samples over time (Fig. S5). Using a mixed linear effects model, we found that Muribaculaceae changed significantly over time in all groups, and was significantly different when comparing control and azithromycin (p value = 0.020). Further, the change over time in the azithromycin group significantly differed from the change in abundance over time in control mice (p value = 0.015). Both groups of antibiotic-exposed mice had increased Verrucomicrobia (*Akkermansia*), and the azithromycin-exposed mice had unique losses within the Firmicutes, mostly Lachnospiraceae species. Azithromycin-exposed mice showed a unique enrichment of *Ileibacterium* in P60 samples that was not observed in amoxicillin or control samples. Samples from the amoxicillin-exposed mice clustered more closely with control samples until P60 but showed reduced *Lactobacillus* abundances compared to both other groups (Fig. 2).

We then assessed whether there were antibiotic-induced compositional differences in the lungs. At P60, but not before, the mice exposed to azithromycin early in life had reduced representation of pulmonary ASVs (Fig. S6A), but there were few other differences in pulmonary microbiota compositions between antibiotic-exposed and control mice (Fig. S6B, C). In total, these data indicate persistent effects on the host microbiome with effects being either conserved across both antibiotics, or antibiotic-specific with the most substantial effects on the colon, cecum, and stomach microbiota composition. Given the antibiotic-induced effects on the host gastrointestinal bacterial communities, we sought to test if altered microbiota composition is involved in host immunomodulation in response to HDM sensitization and challenge.

Role of the altered microbiome in the immunological phenotypes of adult mice

We next asked whether the compositional differences in the intestinal microbiota directly led to an altered immune response to HDM. To address this question, we experimentally transferred microbiota collected from P25 mice (15 days after the antibiotic exposure had ceased) into 6–8-week-old germ-free mice (Fig. 3a). P25 was selected as the timepoint of transfer to ensure that fecal pellets did not contain any residual antibiotics, and that it was early enough in development to permit a maturation of the transferred microbial community in the new murine host. The fecal pellets used for transfer were either perturbed by the prior antibiotic exposure or from control mice (no antibiotic exposure). Consistent with the timeline of the initial studies, 45 days post-transfer, the mice were sensitized and challenged with HDM or PBS and sacrificed at post-transplant day 60 to evaluate immune responses. Apart from a rise in BAL cellularity in the mice that received the amoxicillin-perturbed microbiota, there were no significant differences observed in serum IgE, BAL cellular composition, or cytokine production by $CD4^+$ T cells in mice that received different microbiota (Fig. S7). These results indicate that conventionalization of germ-free adult mice with perturbed microbiota was not sufficient to transfer any phenotype previously

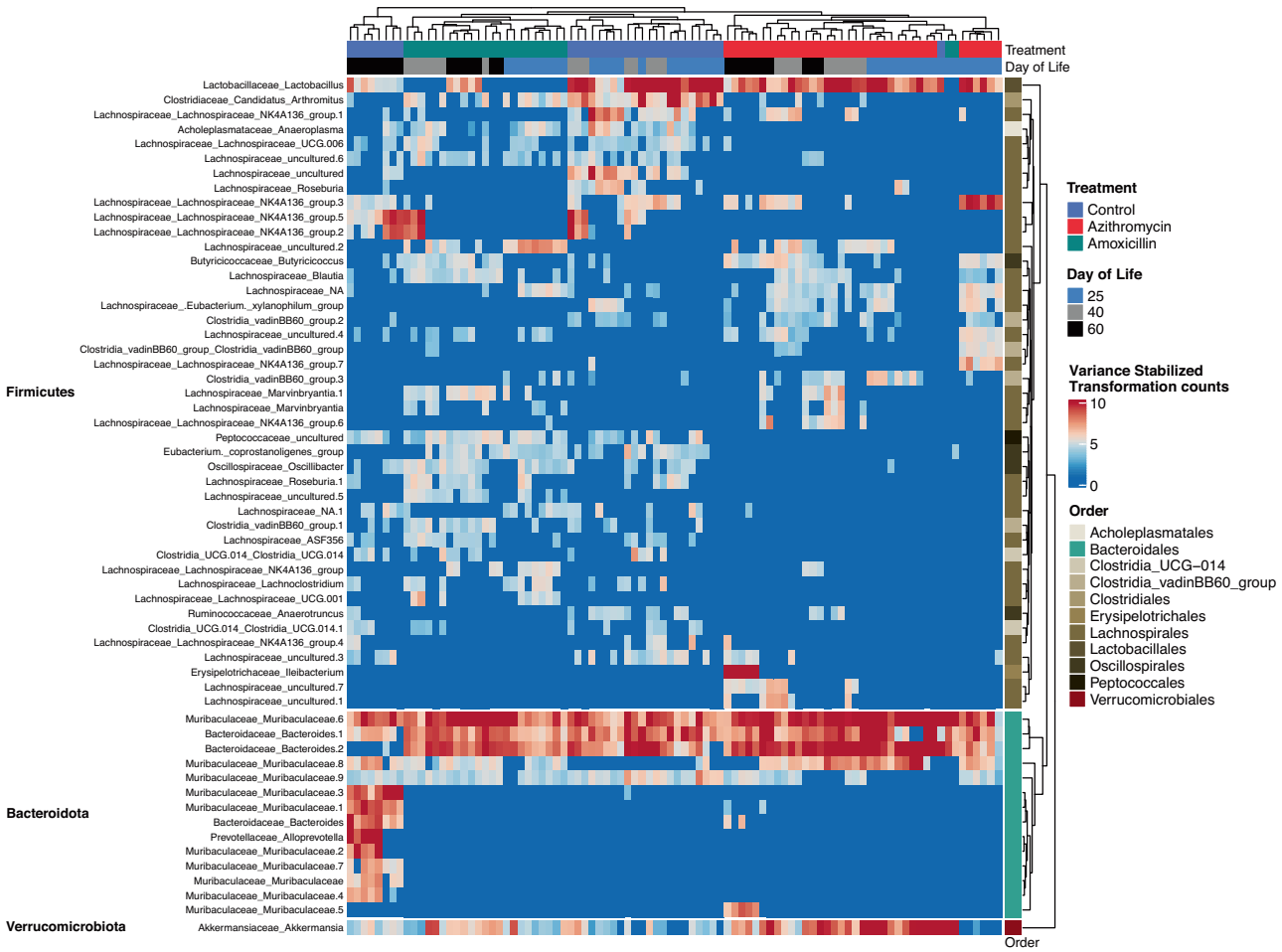

Fig. 2 Identifying significantly altered ASVs between control and antibiotic-exposed mice. Unsupervised hierarchical clustering of differentially abundant ASVs from 92 fecal samples (columns) from 42 individual mice across multiple timepoints, identified using DESeq2, with false discovery rate (FDR) set to $p < 0.01$. Samples are color-coded by treatment, day of life, and body site. Rows indicate statistically significant taxa ($n = 58$), taxa annotation at the genus level (species level information also included when available, annotated as: genus_species).

observed in SPF-conventional mice exposed to antibiotics during the neonatal period (Fig. S1). One explanation for this finding is that there is an age-window during which the immune system is most sensitive to perturbations in intestinal microbiota.

Role of the altered microbiome in the immunological phenotypes of mice exposed from birth

To address the possibility of an age-dependent variable, we assessed immunological responses to HDM in mice exposed to the perturbed microbiota from birth (Fig. 3a). From within the original group of conventionalized germ-free adult mice, some animals were used for antigen challenge (described above), but others were used for breeding. As such, their offspring acquired either a perturbed or control fecal microbiota from birth via vertical transmission. First, to determine if there were any differences in bacterial abundance based on mode of microbiota acquisition, we quantified 16S copy number in the fecal samples from the original SPF cohort, the germ-free adults that were gavaged with fecal samples, and the progeny of the germ-free mice (Fig. 3b). We found no differences in 16S copy number between the experimental groups. To assess the compositional fidelity of the transferred perturbed or control microbiota, we compared the relative abundances of all annotated genera between the SPF donor, germ-free adult recipient, and the resultant offspring mice in each group (Fig. 3c). These analyses showed significant correlation of the taxa present in donor and gavaged adult mice, and donor and offspring mice, indicating high fidelity transfer (Fig. 3c), and that the correlation strength (Spearman rho) was favorable ($\rho > 0.4$) in all cases. These analyses were conducted on samples from multiple experiments and sequencing runs, subject to batch effects which could skew the comparison between samples. The greatest fidelity between the experimental generations involved transfer of the control microbiota, and less so for the antibiotic-perturbed microbiota. This may be an indication of reduced community resiliency and stability, confirming prior observations[27]. This reduced resiliency may factor into the diversity loss observed in the transfer of the antibiotic-perturbed microbiota within fecal samples.

Based on these transfers, we had a way to generate offspring mice that had not received antibiotics themselves but were exposed to the perturbed microbiota from birth (Fig. 3a). Using the same HDM allergen model and measurements of immunity, we assessed if these animals would mirror the effects of directly administered antibiotics in terms of heightened IgE and IL-13 responses. The mice that had an azithromycin-altered microbiota from birth had higher serum IgE concentrations than control mice, after HDM sensitization and challenge (Fig. 4a) which also was observed in the SPF mice following the early-life azithromycin exposure (Fig. S1D). Following HDM challenge, the mice colonized with the azithromycin-perturbed microbiota also had increased BAL cellularity and eosinophil and

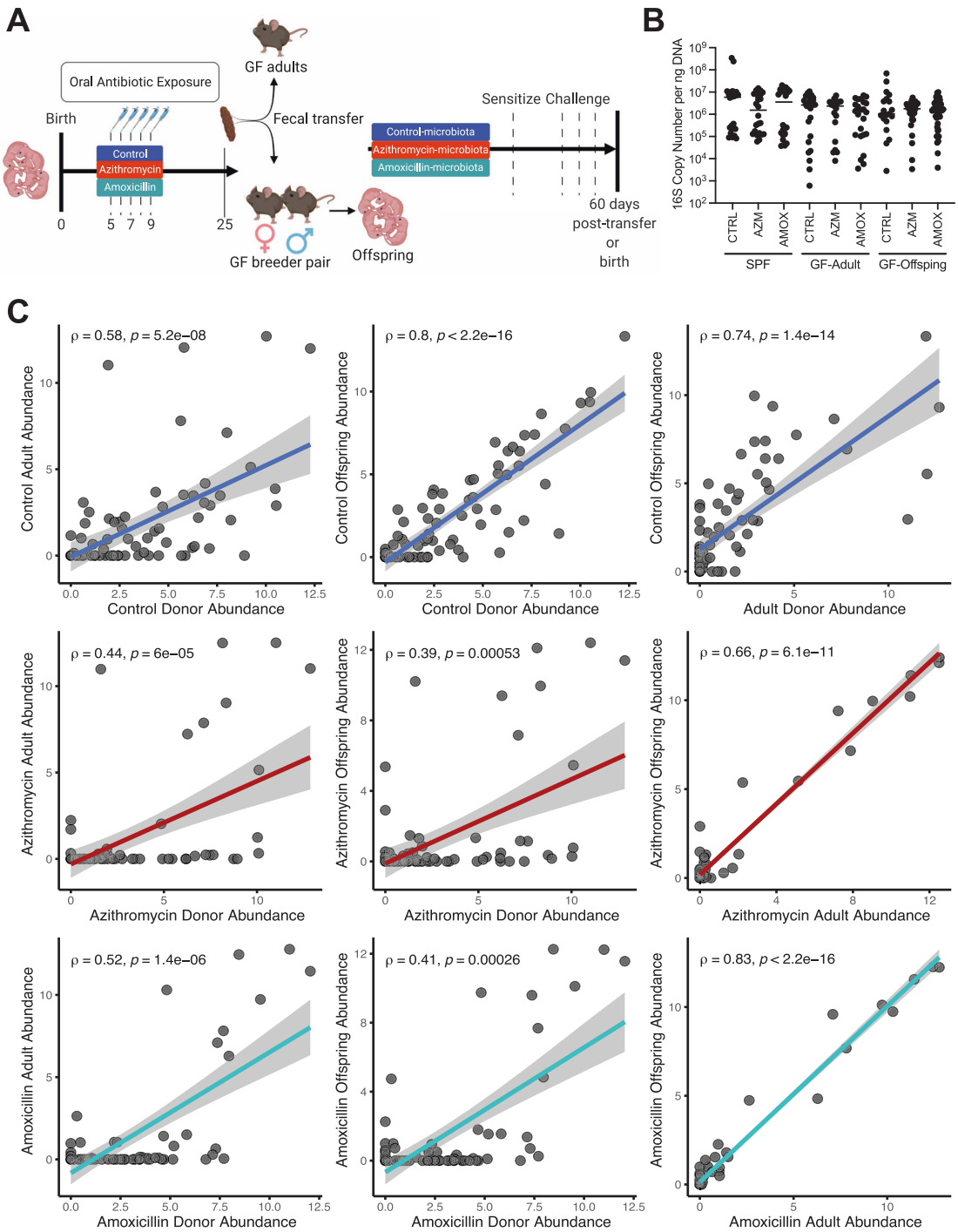

Fig. 3 Differential microbiota in experiments conventionalizing germ-free mice. a Adult (6–8-week-old) germ-free mice were conventionalized with a suspension of fecal microbiota prepared from frozen P25 fecal samples collected from SPF mice varying in antibiotic-exposure (Figs. 1 and 2, and this figure). A subset ($n = 6$–8) of these mice were evaluated for immune responses to HDM through sensitization and challenge with antigen or to PBS. Other conventionalized mice ($n = 3$ per donor) were used as breeder pairs to provide progeny exposed to the conventionalized microbiota from birth. **b** 16S rRNA copy number was determined using qPCR, and copy number was normalized to the total DNA concentration of the sample and reported as copy number per ng of DNA. Fecal samples for day of life/day post gavage 25, 40, and 60 were analyzed for copy number. **c** Spearman correlations between donor SPF mice, adult germ-free mice gavaged with stool and conventionalized offspring mice (3A) for all three experimental groups. Each point represents the $\log_2$ abundance of a unique taxon at the genus level within each experimental group of mice. All identified genera were included ($n = 74$). The correlations strength (Spearman rho) was positive ($\rho > 0.4$ in all cases), and significant ($p < 0.001$) in all comparisons. Sequencing data were pooled from three sequencing runs, and multiple experiments.

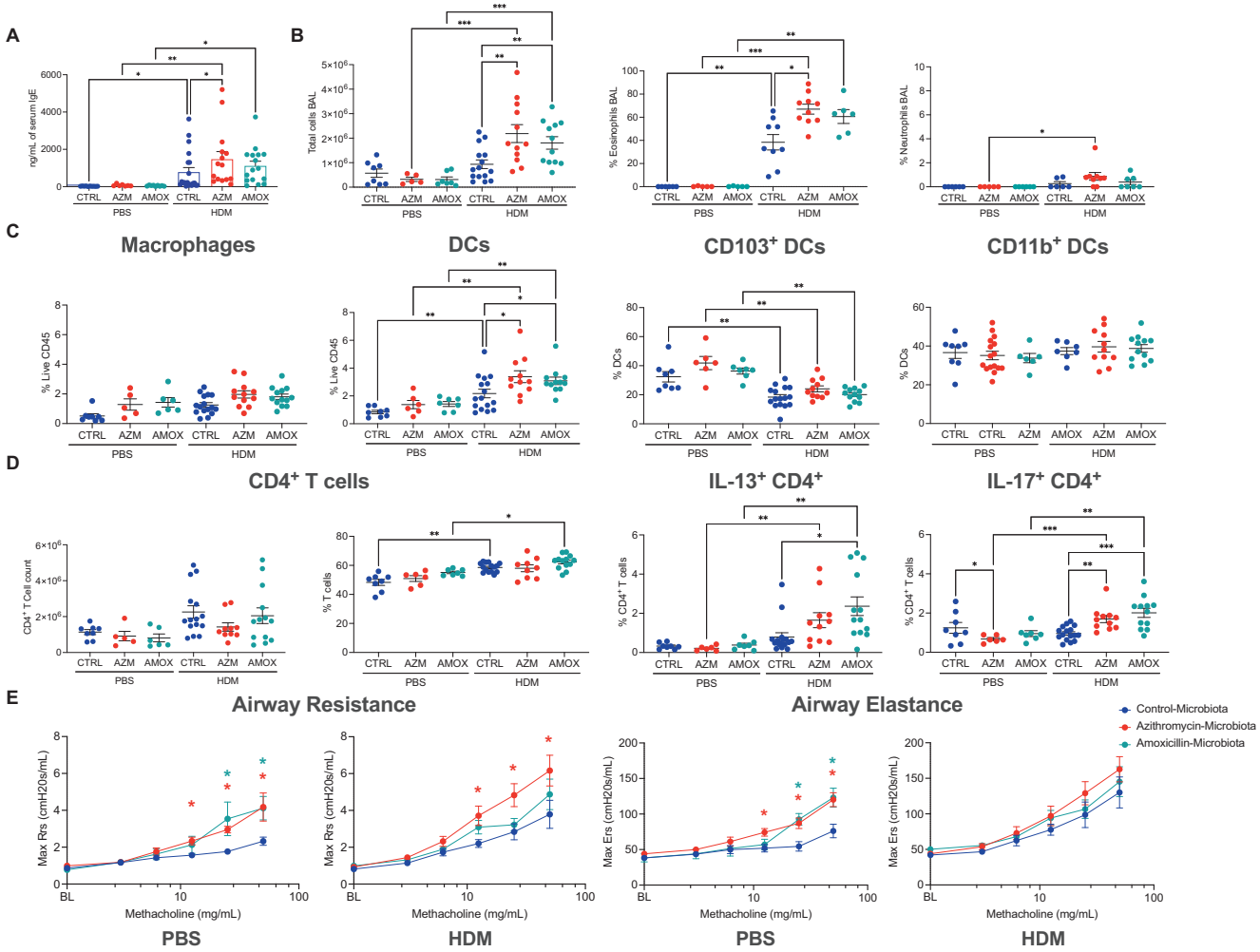

Fig. 4 Phenotypes in the progeny of parental germ-free mice conventionalized with antibiotic-perturbed microbiota. Progeny of germ-free mice that had been conventionalized with the fecal microbiota of antibiotic-exposed or control SPF mice (see Fig. 3a) were evaluated at sacrifice for immune responses to HDM antigen. **a** Serum IgE levels were determined by IgE-specific ELISA. **b** BAL was evaluated for total cell counts by trypan blue staining, or after BAL samples were cytocentrifuged and differentially stained, for proportion of eosinophils, or neutrophils. Lung single cell suspensions were isolated and evaluated by flow cytometry for differences in the **c** myeloid compartment or **d** stimulated ex vivo using PMA and ionomycin. Data were collected from three independent experiments; each individual experiment yielded the same trend. Subsets of the offspring mice were evaluated for differences in lung function by methacholine challenge assay, using a Scireq FlexiVent apparatus. Offspring mice sensitized and challenged with HDM or PBS were evaluated for **e** airway resistance and airway elastance in response to increasing methacholine doses (PBS, $n = 5–8$ per group and HDM, $n = 10–12$ per group, data are from three independent experiments). *$p < 0.05$; **$p < 0.01$; ***$p < 0.001$, ****$p < 0.0001$; nonparametric one-way ANOVA.

neutrophil proportions (Fig. 4b) and had higher proportions of dendritic cells (Fig. 4c). We did not observe changes in infiltration or frequencies of $CD4^+$ T cells associated with receipt of either antibiotic-perturbed-microbiota (Fig. 4d). We did observe significant increases in $CD4^+$ T cells producing IL-17A in mice that received either azithromycin or amoxicillin-perturbed microbiota, and IL-13 in mice that received the amoxicillin-perturbed microbiota (Fig. 4d). The mice exposed to the amoxicillin-perturbed microbiota from birth did not have altered IgE levels, like the amoxicillin-exposed SPF mice, but had increased total number of BAL cells and increased proportions of pulmonary dendritic cells (Fig. 4a, b and Fig. S1D). In total, this experiment demonstrates that acquiring an antibiotic-perturbed microbiota from birth leads to allergen-induced immunological hyperactivity.

Physiologic consequences of exposure to an antibiotic-perturbed microbiota

Finally, we sought to determine whether the observed immunological changes had physiological consequences related to asthma risk or severity. We addressed this question using experimental methacholine challenges to assess bronchial airway reactivity in the mice exposed to control or the altered microbiota from birth and subjected to HDM or PBS challenge (Fig. 3a). The mice exposed from birth to either of the two antibiotic-perturbed microbiota and challenged with PBS showed higher airway reactivity measured by both maximal resistance and elastance (Fig. 4e). As expected[28], both airway resistance and elastance in response to increasing doses of methacholine were significantly greater in all mice that had prior HDM challenge than in those PBS-challenged. Among the HDM-challenged mice, those exposed to the azithromycin-perturbed microbiota from birth had significantly greater airway resistance than mice exposed to the control microbiota; exposure to the amoxicillin-perturbed microbiota had little effect (Fig. 4e). There were no significant differential effects on airway elastance among the HDM sensitized and challenged mice, but the antibiotic-perturbed microbiota mice had higher airway elastance relative to control among the PBS challenged mice (Fig. 4e). In total, these experimental findings

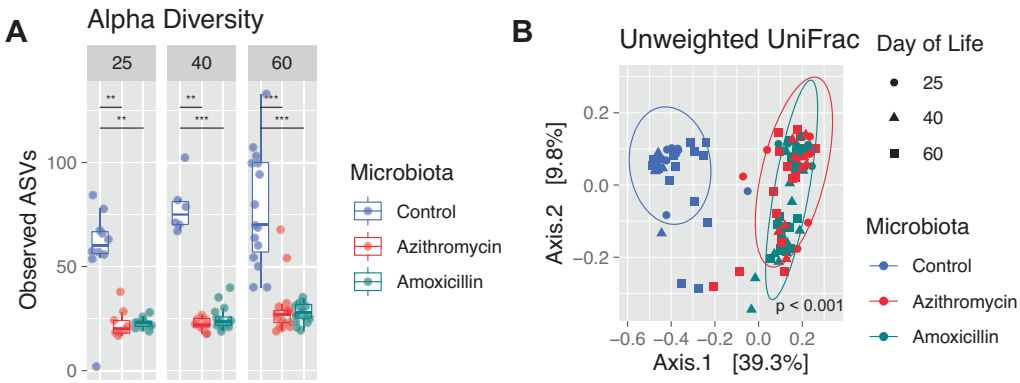

Fig. 5 Altered alpha and beta diversity in mice that had an antibiotic-perturbed or control microbiota from birth. a Alpha diversity across P25, P40 and P60 for each group of mice based on birth-microbiota. Significance for alpha diversity was determined by a nonparametric one-way ANOVA (*$p < 0.05$; **$p < 0.01$; ***$p < 0.001$). **b** Beta diversity, based on unweighted UniFrac analysis of P25, P40, P65 fecal pellets. Each sample is color-coded by microbiota group and symbols are used to differentiate day of life. Permutational multivariate analysis of variance was performed to compare microbiota, day of life, and the interaction of both factors (p value <0.001); 41% of variance could be attributed to the founding microbiota source; 3.5% of variance could be attributed to day of life, and 3.3% of variance was attributed to both microbiota source and day of life.

provide evidence that exposure to antibiotic-perturbed microbiota from birth affects pulmonary physiological function with and without allergen challenge. These results experimentally link antibiotic-perturbed early-life microbiota to allergic predisposition, heightened immunological responses to allergen, and clinical features of allergic asthma.

Microbiota composition associated with altered immune phenotypes

To characterize differences in microbiota composition of the mice that were born with control or antibiotic-perturbed microbiota, 16S rRNA sequencing was employed. Analysis of observed ASVs (Fig. 5a) revealed that mice with the antibiotic-perturbed microbiota had significantly reduced alpha diversity relative to control animals and did not show the increases in observed ASVs with maturation that were seen in controls. An unweighted UniFrac analysis showed clear and significant differences in fecal community composition between control-microbiota mice and antibiotic-perturbed microbiota mice (Fig. 5b). Differentially abundant ASVs are highlighted in Fig. S8, with the mice exposed to the antibiotic-perturbed microbiota having increased abundances of *Akkermansia*, *Muribaculum*, *Bacteroides*, *Lachnostridium*, and *Blautia*. Many of these ASVs are consistent with differentially abundant taxa identified in the SPF experiments (Fig. 2). To further highlight consistently altered colonic ASVs associated with antibiotic exposure in these experiments, ASVs that were differentially abundant between controls and azithromycin-perturbed mice from both the SPF experiments (Fig. 1a) and the transfer experiments (Fig. 3a) from P25 and P60 are identified in Tables S1 and S2, respectively. Table S1 identifies potentially important ASVs during early-life (P25) which include segmented filamentous bacteria (SFB; *Candidatus Arthomitus*), *Akkermansia*, Oscillospirales, and Muribaculaceae species. All apart from *Akkermansia*, were enriched in control mice. Later at P60, Muribaculaceae and Oscillospirales continue to be present in increased abundance in control mice, and Lachnospiraceae and Clostridia also show higher representation in control mice relative to the azithromycin-perturbed microbiota mice. Parabacteroides was the only ASV overrepresented in azithromycin-microbiota mice at P60 in both sets of experiments. These data provide evidence that the mice that were exposed from birth to antibiotic-perturbed microbiota had clear compositional differences, and reduced diversity relative to control-microbiota animals.

Next, to determine ASVs that may be associated with the immune phenotypes observed in the microbiota transfer experiments, we correlated lung IL-13 and IL-17A production by $CD4^+$ T cells to ASVs that significantly differed between recipient mice that received control or antibiotic-perturbed microbiota. Non-hierarchical clustering of significantly correlated ASVs ($p < 0.05$) revealed that there are distinct microbial signatures in the control and antibiotic-perturbed microbiota groups that correlate with both IL-13 and IL-17A production (Fig. 6a, b). Many Lachnospiracae and Muribaculaceae strains were enriched in control mice and negatively correlated with cytokine production. *Akkermansia* and some Tannerellaceae strains had higher relative abundance in the mice receiving the antibiotic-perturbed microbiota and significantly correlated with elevated cytokine production (Fig. 6a, b). We also tested correlations between ASV relative abundance and total BAL counts, lung eosinophilia, and serum IgE without identifying any significant associations or clear compositional differences. In total, these data indicate that there are compositional differences associated with the $CD4^+$ T cell phenotypes in this study. Further, the germ-free experiments permitted the transfer of compositional microbiome differences found in SPF antibiotic-exposed mice into new hosts, and showed that germ-free mice that developed with the perturbed microbiota from birth had altered immune and physiological responses to HDM.

DISCUSSION

Our data indicate that direct administration of either of the two most commonly prescribed antibiotics in pediatric practice[6,16,17] to murine pups causes sustained differences in gastrointestinal microbial communities, extending prior studies with antibiotic administration in drinking water that exposes both dams and pups[18,19,26]. This was evident by the unweighted UniFrac analysis of stomach, cecum, and fecal samples of the antibiotic-treated mice which indicated long-term compositional differences; alpha-diversity was largely restored by the time of sacrifice (Fig. 1b–e). Interestingly, although dams remained untreated in our studies, we still found sustained differences in the gastrointestinal microbiota of the antibiotic-exposed pups into adulthood. This reveals that there was not a substantial restoration of the pup microbiome from their mom to resemble an untreated mouse. This is consistent with prior work in which co-housing control and antibiotic exposed mice did not rescue microbiota-dependent immune phenotypes or restore microbiome composition[26,29]. This work provides experimental evidence consistent with the epidemiological data that early-life antibiotic use is associated

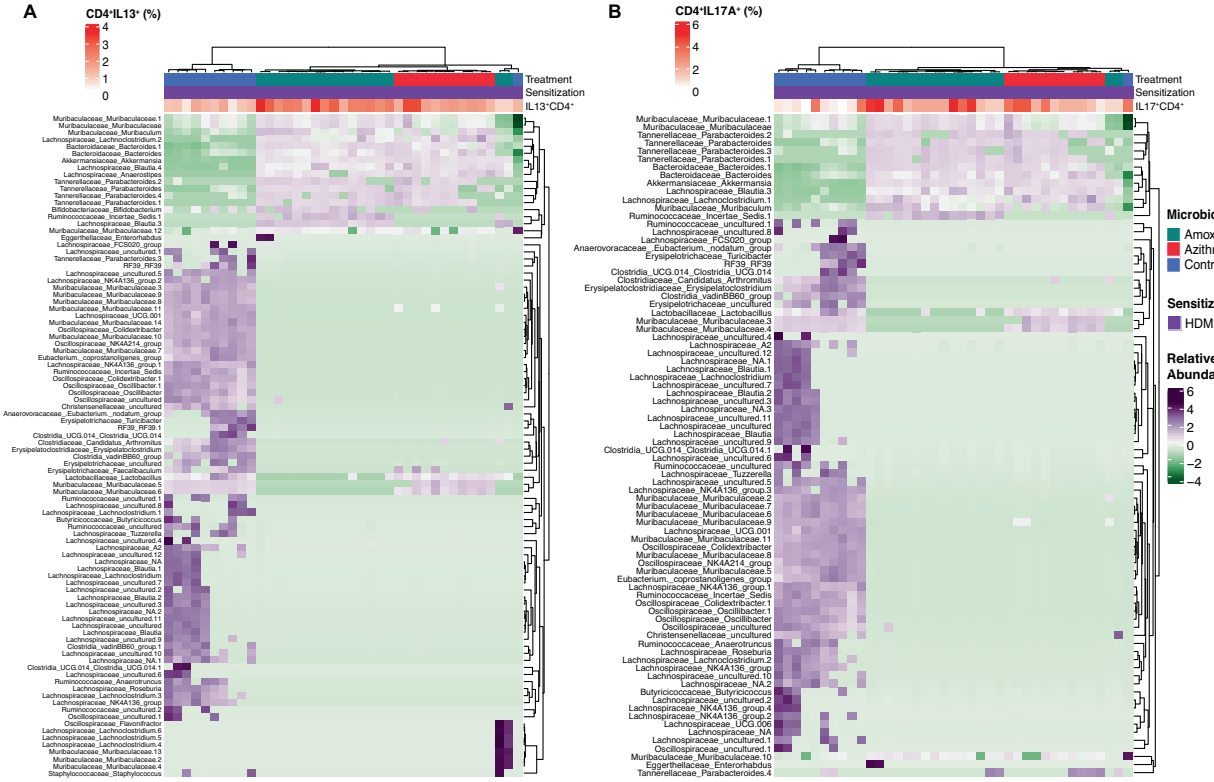

Fig. 6 ASVs in the progeny mice conventionalized with antibiotic-perturbed microbiota correlate with elevated CD4$^+$ T cell production of IL-13 and IL-17A. Spearman correlations were used identify the colonic ASVs from the offspring-recipient mice sensitized and challenged with HDM (Fig. 4a) that significantly correlate with lung CD4$^+$ T cell production of **a** IL-13 and **b** IL-17A. Each row is an ASV that is significantly correlated with the frequency of cytokine produced by pulmonary Th cells. ASVs were considered based on nominal significance ($p < 0.05$). The heatmap includes 39 colonic samples from 22 unique mice all of which were sensitized and challenged with HDM. Samples are annotated by source of microbiota, sensitization, timepoint at which the sample was collected, and the body site (colon or fecal pellet). The heatmap is colored by scaled (*z*-score) ASV relative abundance.

with increased risk of asthma and related allergic diseases in children later in their life[6–8,30]. We found that azithromycin exposure during early-life heightened IgE and lung CD4$^+$ T cell IL-13 production. That treatment of germ-free mice with antibiotics had no effect on allergen-specific immune responses indicates that the antibiotic effects require the presence of a microbiota as an intermediate. This is consistent with earlier studies, which found that treatment with the macrolide tylosin altered the immunological status of mice, but when germ-free mice were treated with tylosin, no immunological effects were observed 19. The lack of effect seen when transplanting the antibiotic-perturbed microbiota into adult germ-free mice, when taken together with the strong observed influence this microbial composition had on mice exposed to this microbiota from birth, provides evidence for a critical age window in which host microbial composition exerts immunomodulatory effects. This is in line with prior observations showing that human infant microbiota composition during the first 100 days of life is a critical determinant of asthma susceptibility[31]. and adds to understanding of an early ontogenic window of opportunity for impacts of the intestinal microbiota on the immune landscape of the lung. This experiment also provides mechanistic evidence for a direct role of the perturbed microbiota in modulating allergy risk and severity, and further rules out direct effects of the antibiotic on host tissues in playing any substantial role.

Although broad spectrum super-therapeutic antibiotic regimens perturb immune dynamics in the lung and elsewhere[32–34], to our knowledge, no other studies have shown that early-life exposure to a single measured antibiotic at therapeutic levels alter the lung cytokine environment following antigen challenge. Similarly, no other studies have shown that clinically relevant doses, durations, and routes of antibiotic exposures were sufficient to alter gut microbial composition in mice for periods >6 weeks, and that microbiota composition was sufficient to alter the immune landscape and pulmonary function. Previous murine studies have shown that super-therapeutic antibiotics resulted in reduced Tregs in the lymph nodes draining the lungs 34. In our studies, there were no observed decreases in frequency or abundance of Tregs or pTregs in the lung tissue of the antibiotic-exposed mice before or after HDM challenge. Our results provide evidence that the antibiotic-driven pulmonary immune changes are not modulated by altered pulmonary Treg numbers but do not rule out functional differences of these T cells, or contributions of gastrointestinal tract-derived Tregs.

Although our studies indicate effects of a perturbed intestinal microbiota as a causal element, we did not examine contributions of viral, bacterial, or fungal infections, which lead to antibiotic prescriptions for children[4,35,36]. We also did not find significant changes in the pulmonary microbiota, although it is known that airway microbial changes may influence asthma pathogenesis in humans[42] and mice[37,38]. The lower airway microbiota has also been associated with the development of wheeze in children[39], and pulmonary microbial signatures were found to cluster based on asthma endotype in adults[40]. Despite no experimental evidence of the pulmonary microbiota influencing our observations, the contributions of the altered intestinal microbiota to the enhanced allergic/inflammatory phenomena were both substantial and consistent in the models we used.

A brief early-life amoxicillin course uniquely and persistently altered the gastric microbiota. Such effects can potentially

influence host immunity, paralleling antibiotic abrogation of *Helicobacter pylori* immunomodulatory properties related to asthma[14,41–43]. Amoxicillin exposure altered IL-17 $CD4^+$ T cell HDM responses, with phenotypes consistent with neutrophilic asthma[44]. Amoxicillin-exposed mice had notable decreases in gastric and colonic *Lactobacillus* and Lachnospiraceae strains relative to controls. In prior murine studies, oral *Lactobacillus* administration reduced inflammation in models of antigen-driven lung inflammation[45,46]. Lachnospiraceae produce the short-chain fatty acid butyrate[47], which was shown to have anti-inflammatory effects in the lungs of OVA-sensitized and challenged mice[32,48,49]. The mechanism for the amoxicillin-induced IL-17-dominanted immune responses to HDM may involve reductions of these important gastric taxa, potentially impacting gastric-derived pTregs, which have been reported to reduce HDM-associated pulmonary inflammation in murine models of *H. pylori* infection[50]. In our own data, we found that increased colonic abundance of Lachnospiraceae was negatively associated with lung $CD4^+$ T cell IL-17 production.

Mice that developed from birth in the presence of the azithromycin-perturbed microbiota had heightened Type 2 and Type 17 immune responses to HDM; the heightened Type 2 responses were also observed in SPF mice exposed to azithromycin during early-life. Azithromycin exposure reduced intestinal alpha-diversity until P40, a finding consistent with the association between reduced 1st-year of life bacterial diversity and higher subsequent asthma risk in human children[51]. Germ-free mice have hyper-IgE responses and increased susceptibility to anaphylaxis; however this can be abrogated through conventionalization with a diverse microbiota during early-life but not later[52]. These data support the hypothesis of a critical window of time for host-microbiota interactions which are dependent on both composition and age. ASVs that significantly correlated with $CD4^+$ T cell cytokine production in the lung tissue of the mice that received antibiotic-perturbed microbiota (Fig. 6) included Muribaculaceae, a family within the phylum Bacteroidetes, and Lachnospiraceae a family within the phylum Firmicutes, which both were reduced. In prior studies, exposure to these phyla over the first 3 years of life negatively correlated with atopy and atopic wheeze in children[53]. Both phyla also contribute to short-chain fatty acid production[54], metabolites that reduce inflammation in other murine asthma models[32,48,49]. Children with the highest levels of butyrate and propionate at 1 year of age are less likely to develop asthma during early childhood[48]. Azithromycin-exposed mice had reduced SFB levels during early-life and enrichment for *Akkermansia*. SFB potently induce Th17 cells[55], loss of this taxon could lead to dysregulation of T cell differentiation and T cell immunity. *Akkermansia* has been shown to bloom following antibiotic treatment in both mice[18,19], and humans[56], and to degrade mucins and generate metabolites including acetate and propionate[57]. Although *Akkermansia* is a biomarker of recent antibiotic exposure, we are not able to conclude from these experiments the functional role of its antibiotic-induced bloom. These data from humans and mice suggest a time window during early-life in which protection against allergic diseases is associated with particular microbial compositions and metabolites. Our transfers to germ-free mice provide direct evidence that this developmental window is a critical variable.

In a Danish cohort, children diagnosed with asthma by age 7 already had decreased air flow and increased methacholine responsiveness at age 1 month compared to children who did not develop asthma later[58]. Similarly, an abnormal microbiota at age 1 year was significantly associated with risk of asthma developing by age 6[59]. Airway resistance in azithromycin-perturbed microbiota mice differing from controls (Fig. 4e) without antigen challenge provides evidence for predisposition to altered lung physiology that is microbiome-dependent. This supports observations in these childhood cohorts[58,59].

In total, our studies indicate a window during early-life, with conserved cross-talk between the assembling gastrointestinal microbiota and the host immune system that supports healthy development[60], but which can be abrogated by therapeutic antibiotic regimens that substantially affect microbiome composition. Despite their many clinical benefits, antibiotics disrupt the conserved early-life mutualism between host and microbes. Further understanding of the mechanisms by which perturbation of this microbiota-immune axis influences predisposition to asthma and other allergic disorders will inform methods in the clinic to mitigate or reverse these processes.

MATERIALS AND METHODS

Mice

C57BL/6J mice were purchased from Jackson Laboratories at New York University School of Medicine, or from Javier at the University of Zürich and acclimated to the animal facility for 1 week prior to breeding. C57BL/6 germ-free mice were obtained from Taconic Biosciences, and maintained in a laminar flow isolator at a germ-free facility at NYU School of Medicine. Mice were maintained on a 12-h light/dark cycle and allowed ad libitum access to rodent standard lab chow and water. For germ-free mice, all food and water were autoclaved. All mouse experiments were approved by the New York University Langone Institutional Animal Care and Use Committee (IACUC protocol IA16-00785) and complied with federal and institutional regulations. All animal experimentation at the University of Zurich was reviewed and approved by the Zurich Cantonal Veterinary Office (licenses ZH170/2014 and ZH086/2020).

Antibiotic treatment

Between P5-9, mice received either sterile water, or an oral suspension of 30 mg/kg of active azithromycin (Teva, Fairfield NJ) or 100 mg/kg of amoxicillin (Sigma, St. Louis MO). Oral suspensions were prepared in sterile water. Mouse pups were weighed, and the volume of the suspension adjusted for each mouse to achieve the desired daily dose, with a new suspension prepared every 48 h. Dams remained untreated in these experiments. For antibiotic treatment of germ-free pups, autoclaved water was used to prepare the antibiotic suspension in a hood with laminar flow, and the suspension was filter-sterilized. New antibiotic suspensions were prepared for each germ-free treatment.

House dust mite (HDM) antigen model

Lyophilized HDM antigen was purchased from Greer (XPB82D3A2.5, Cambridge MA) and dissolved in sterile PBS (Corning, Oneonta NY) at a concentration of 2 mg/ml based on total protein concentration. At P45, offspring mice were sensitized intranasally with 1 ug of HDM in 50 ul PBS, or with PBS alone as a negative control. On P53, P55 and P57, mice were challenged intranasally with 10 ug of HDM in 50 ul PBS, or with PBS alone as a negative control. On P60, mice were euthanized, blood was collected by cardiac puncture, and the lungs perfused with PBS. Gastrointestinal tract samples were snap-frozen on dry ice and stored at −80 °C.

BAL collection

After tracheotomy and insertion of an 18-gauge cannula, BAL was collected. Total viable cells were counted by trypan blue dye exclusion, and differential cell counts were performed on cytocentrifuged samples stained with Shandon Kwik-Diff Stains (Thermo Scientific, Springfield Township NJ).

Lung histology

For histopathology, lungs were fixed by means of inflation and immersion in 4% formalin and embedded in paraffin. Tissue sections were stained with hematoxylin and eosin or periodic acid–Schiff (PAS). Images were evaluated blindly using a BX40 Olympus microscope (Olympus, Center Valley PA). Peribronchial inflammation was scored from 0–4. PAS-positive goblet cells were quantified per millimeter of basal membrane on at least three different representative airways on PAS-stained slides. More detailed information on scoring has been described previously[61].

IgE ELISA

The left lung was collected and homogenized in T-PER tissue protein extraction reagent (Thermo Scientific) supplemented with Halt protease

and phosphatase inhibitors (Thermo Scientific) to extract total protein. ELISA MAX Deluxe set mouse total IgE (BioLegend, San Diego CA) was used to quantify IgE levels in both serum and lung tissue homogenate. Lung tissue homogenate immunoglobulin concentrations were normalized to the total protein levels in the sample, quantitated by BCA assay (Pierce, Springfield Township NJ).

Flow cytometry

At mouse sacrifice, the middle lung lobe was perfused with PBS, excised, minced into small pieces using dissection scissors and submerged in DMEM (Corning) supplemented with 10% fetal calf serum (FCS) (Corning) and penicillin and streptomycin (Corning). Lungs were enzymatically digested in DMEM supplemented with 10% FCS, 0.5 mg of Collagenase 1A (Sigma, United States) and 0.05 mg of DNase I (Worthington Biochemical, Lakewood, NJ) for 35 min at 37 °C with shaking and were subsequently mechanically disrupted. Lung suspensions were passed through a 70-micron filter (Milltenyi, Sommerville MA). For stimulation experiments, lung cell suspensions were cultured for 4 h at 37 °C in RPMI supplemented with PMA (Sigma), ionomycin (Sigma), golgi plug (BD), 10% FCS, beta mercaptoethanol, and penicillin/streptomycin. Cell suspensions were stained with fluorescently tagged antibodies (BioLegend San Diego, CA; BD Franklin Lakes, NJ; and eBiosciences San Diego, CA). All data were acquired on a BD LSRII flow cytometer at the NYU School of Medicine Flow Cytometry Core or a BD Fortessa at the University of Zurich Flow Cytometry Core. All data were analyzed using FlowJo (v10.6.1, BD). Count bright beads (Invitrogen) were used to determine cell counts in flow cytometry experiments.

FlexiVent and methacholine challenge

Mice were anesthetized with a cocktail of ketamine and xylazine, tracheotomized and a 20-gauge metal cannula was inserted into the trachea and connected to the computer-operated animal ventilator (FlexiVent, Scireq, Montreal, Canada). Mice were mechanically ventilated and baseline measurements recorded based on standard Scireq protocols[62]. A nebulizer was used to aerosolize PBS or increasing doses of methacholine (Sigma) were delivered to the mouse, and airway resistance measured. A dose response curve was generated using methacholine at doubling doses from 3.125 to 50 mg/ml.

DNA isolation and 16S rRNA sequencing

DNA was extracted from gastrointestinal samples with the DNeasy PowerSoil HTP 96 Kit (Qiagen, Germantown MD) or DNeasy PowerLyzer Powersoil kit (Qiagen). DNA was extracted from lung lobes using a DNeasy Blood and Tissue Kit (Qiagen). PBS, HDM, and no sample controls also were extracted to assess for background bacterial contamination of lung samples. The V4 region of the bacterial 16S rRNA gene was amplified in triplicate, using barcoded fusion primers (F515/R806)[63], then pooled, and DNA was quantified with Quant-iT PicoGreen (Invitrogen, Springfield Township, NJ). A maximum of 96 samples were then pooled in equal quantities of 300 ng, and then purified with a QIAquick PCR purification kit (Qiagen) and quantified with a Qubit Fluorometer (Life Technologies, Springfield Township, NJ). Finally, these samples were pooled at an equal molar concentration (50 nM) and sequenced on an Illumina MiSeq platform at the New York University School of Medicine Genome Technology Center. All data were processed and analyzed using Quantitative Insights into Microbial Ecology (QIIME2, version 2020.02)[64]. Sequencing reads were trimmed and denoised using DADA2[65] and aligned using MAFFT[66]. Taxonomy was assigned using Silva 138 (released December 2019), cyanobacteria, mitochondrial, and chloroplast sequences were removed, and only ASVs that were present in ≥10 samples and had a total count >15 across all samples were included in subsequent analyses. For the SPF experiments, 416 samples were included at a sequencing depth of 5.8 million reads with an average number of reads per sample of 13,527 (range 5042–84,746). For the GF-transfer experiments, 285 samples were included at a sequencing depth of 5.6 million reads, at an average number of reads per sample of 18,773 (range 8962–99,359). Beta diversity (unweighted UniFrac) analyses, rarefied at 5000 reads, were performed using the QIIME2 pipeline, and plots were generated in R using ggPlot2. Alpha diversity (Observed ASVs) and taxonomic abundance plots were generated using the Phyloseq package, and differential abundance plots and heatmaps were generated using the DESeq2 and Complex Heatmap packages in R[67,68]. Lung 16S rRNA samples were subject to background subtraction prior to analysis using the prevalence method of the Decontam open source R package using the conservative threshold of 0.5[69]. The pipeline was used to remove contaminant ASVs found in background control samples (extraction blank, PCR negative control, PBS and HDM samples) from true lung samples. 16S copy number was determined in DNA samples by qPCR using SyberGreen (Applied Biosystems) and universal 16S primers 785F/907R, and normalized to the DNA concentration determined by the Quant-iT PicoGreen assay. A standard curve using a plasmid that contains the 16S rRNA gene from *Propionibacterium acnes* was used to determine 16S rRNA copy number.

Fecal transfer to germ-free mice

Selected frozen mouse fecal pellets (25 mg) were suspended in 1 ml of Beef Broth medium (10.0 g Beef Extract, 10.0 g Peptone, 5.0 g NaCl in 1.0 l of water, pH 7.2), then disrupted by passage through a 1 ml sterile syringe without needle attached, vortex-mixed, and immediately used for gavage into recipient mice. Sterile disposable 18G gavage needles (Fine Science Tools, Foster City CA) were used to transfer fecal suspensions to conventionalize germ-free mice. Fecal samples were collected periodically to determine engraftment and stability of the community over time.

Statistical analyses

Statistical analysis was performed with Prism 9.2.0 (GraphPad Software). Statistical comparisons between groups were performed using a Kruskal–Wallis test (one-way nonparametric ANOVA). To determine statistical significance between HDM sensitized and challenged mice, the matching PBS group was used as the reference for comparison: control vs. control; azithromycin vs. azithromycin; amoxicillin vs. amoxicillin. This was based on the a priori assumption that antibiotic treatment alone is sufficient to disrupt the immune status of HDM naïve mice[19]. Differences were considered statistically significant when $p < 0.05$. Statistical significance between community structures was determined using an Adonis test and reported as significant when $p < 0.01$. Differentially abundant ASVs were determined by contrasting the relevant treatment groups and selecting for ASVs that were significant using a Benjamini Hochberg false discovery rate of $p < 0.01$. Spearman correlations between all detectable genera between the donor, adult and offspring mice were used to detect the fidelity of microbiota transfer. This analysis considers all detectable bacteria genera and their group average relative abundance (e.g., the mean of each genus in each experimental group of mice). Correlations of the relative abundance of the genera were then conducted between donor and transfer groups to allow for evaluation of transfer strength ($|\rho| > 0.4$) and significance ($p < 0.05$).

DATA AVAILABILITY

The data are available at the following link https://qiita.ucsd.edu/study/description/14608.

REFERENCES

1. Braman, S. S. The global burden of asthma. *Chest* **130**, 4S–12S (2006).
2. Svenningsen, S. & Nair, P. Asthma endotypes and an overview of targeted therapy for asthma. *Front. Med.* **4**, 158 (2017).
3. Wenzel, S. E. Asthma phenotypes: the evolution from clinical to molecular approaches. *Nat. Med.* **18**, 716–725 (2012).
4. Sugita, K., Sokolowska, M. & Akdis, C. A. Key points for moving the endotypes field forward. *Implementing Precision Medicine in Best Practices of Chronic Airway Diseases* (eds Agache, I. & Hellings, P.) 107–114 (Elsevier, Academic Press: London, 2019).
5. Choy, D. F. et al. TH2 and TH17 inflammatory pathways are reciprocally regulated in asthma. *Sci. Transl. Med.* **7**, 301ra129 (2015).
6. Metsälä, J. et al. Prenatal and post-natal exposure to antibiotics and risk of asthma in childhood. *Clin. Exp. Allergy* **45**, 137–145 (2015).
7. Aversa, Z. et al. Association of infant antibiotic exposure with childhood health outcomes. *Mayo Clin. Proc.* **96**, 66–77 (2020).
8. Kozyrskyj, A. L., Ernst, P. & Becker, A. B. Increased risk of childhood asthma from antibiotic use in early life. *Chest* **131**, 1753–1759 (2007).
9. Risnes, K. R., Belanger, K., Murk, W. & Bracken, M. B. Antibiotic exposure by 6 months and asthma and allergy at 6 years: findings in a cohort of 1,401 US children. *Am. J. Epidemiol.* **173**, 310–318 (2011).
10. Patrick, D. M. et al. Decreasing antibiotic use, the gut microbiota, and asthma incidence in children: evidence from population-based and prospective cohort studies. *Lancet Respir. Med.* **8**, P1094–1105 (2020).

11. Ahmadizar, F. et al. Early-life antibiotic exposure increases the risk of developing allergic symptoms later in life: a meta-analysis. *Allergy* **73**, 971–986 (2018).
12. Metsälä, J. et al. Mother's and offspring's use of antibiotics and infant allergy to cow's milk. *Epidemiology* **24**, 303–309 (2013).
13. Sun, W., Svendsen, E. R., Karmaus, W. J., Kuehr, J. & Forster, J. Early-life antibiotic use is associated with wheezing among children with high atopic risk: a prospective European study. *J. Asthma* **52**, 647–652 (2015).
14. Borbet, T. C., Zhang, X., Muller, A. & Blaser, M. J. The role of the changing human microbiome in the asthma pandemic. *J. Allergy Clin. Immunol.* **144**, 1457–1466 (2019).
15. Thomas, M. et al. Atopic wheezing and early life antibiotic exposure: a nested case–control study. *Pediatr. allergy Immunol.* **17**, 184–188 (2006).
16. Chai, G. et al. Trends of outpatient prescription drug utilization in US children, 2002-2010. *Pediatrics* **130**, 23–31 (2012).
17. Hales, C. M., Kit, B. K., Gu, Q. & Ogden, C. L. Trends in prescription medication use among children and adolescents-United States, 1999-2014. *JAMA* **319**, 2009–2020 (2018).
18. Nobel, Y. R. et al. Metabolic and metagenomic outcomes from early-life pulsed antibiotic treatment. *Nat. Commun.* **6**, 7486 (2015).
19. Ruiz, V. E. et al. A single early-in-life macrolide course has lasting effects on murine microbial network topology and immunity. *Nat. Commun.* **8**, 518 (2017).
20. Bokulich, N. A. et al. Antibiotics, birth mode, and diet shape microbiome maturation during early life. *Sci. Transl. Med.* **8**, 343ra382 (2016).
21. Kemppainen, K. M. et al. Association between early-life antibiotic use and the risk of islet or celiac disease autoimmunity. *JAMA Pediatr.* **171**, 1217–1225 (2017).
22. Lynn, M. A. et al. Early-life antibiotic-driven dysbiosis leads to dysregulated vaccine immune responses in mice. *Cell Host Microbe* **23**, 653–660 (2018).
23. Roubaud-Baudron, C. et al. Long-term effects of early-life antibiotic exposure on resistance to subsequent bacterial infection. *mBio* **10**, e02820-19 (2019).
24. Zhang, X.-S. et al. Antibiotic-induced acceleration of type 1 diabetes alters maturation of innate intestinal immunity. *Elife* **7**, e37816 (2018).
25. Gasparrini, A. J. et al. Persistent metagenomic signatures of early-life hospitalization and antibiotic treatment in the infant gut microbiota and resistome. *Nat. Microbiol.* **4**, 2285–2297 (2019).
26. Zhang, X. et al. An antibiotic-impacted microbiota compromises the development of colonic regulatory T cells and predisposes to dysregulated immune responses. *Mbio* **12**, e03335-20 (2021).
27. Schulfer, A. F. et al. Intergenerational transfer of antibiotic-perturbed microbiota enhances colitis in susceptible mice. *Nat. Microbiol* **3**, 234–242 (2018).
28. Piyadasa, H. et al. Biosignature for airway inflammation in a house dust mite-challenged murine model of allergic asthma. *Biol. Open* **5**, 112–121 (2016).
29. Schulfer, A. F. et al. The impact of early-life sub-therapeutic antibiotic treatment (STAT) on excessive weight is robust despite transfer of intestinal microbes. *ISME J.* **13**, 1280–1292 (2019).
30. Ahmadizar, F. et al. Early life antibiotic use and the risk of asthma and asthma exacerbations in children. *Pediatr. Allergy Immunol.* **28**, 430–437 (2017).
31. Arrieta, M.-C. et al. Early infancy microbial and metabolic alterations affect risk of childhood asthma. *Sci. Transl. Med.* **7**, 307ra152 (2015).
32. Cait, A. et al. Microbiome-driven allergic lung inflammation is ameliorated by short-chain fatty acids. *Mucosal Immunol.* **11**, 785–795 (2018).
33. Ichinohe, T. et al. Microbiota regulates immune defense against respiratory tract influenza A virus infection. *Proc. Natl Acad. Sci. USA* **108**, 5354–5359 (2011).
34. Adami, A. J. et al. Early-life antibiotics attenuate regulatory T cell generation and increase the severity of murine house dust mite-induced asthma. *Pediatr. Res.* **84**, 426–434 (2018).
35. Almqvist, C., Wettermark, B., Hedlin, G., Ye, W. & Lundholm, C. Antibiotics and asthma medication in a large register-based cohort study—confounding, cause and effect. *Clin. Exp. Allergy* **42**, 104–111 (2012).
36. Arrieta, M.-C. et al. Associations between infant fungal and bacterial dysbiosis and childhood atopic wheeze in a nonindustrialized setting. *J. Allergy Clin. Immunol.* **142**, 424–434. e410 (2018).
37. Taylor, S. L. et al. Inflammatory phenotypes in patients with severe asthma are associated with distinct airway microbiology. *J. Allergy Clin. Immunol.* **141**, 94–103 (2018). e115.
38. Hanashiro, J. et al. Schizophyllum commune induces IL-17-mediated neutrophilic airway inflammation in OVA-induced asthma model mice. *Sci. Rep.* **9**, 1–9 (2019).
39. Wu, L. et al. Follow-up study of airway microbiota in children with persistent wheezing. *Respir. Res.* **22**, 213 (2021).
40. Abdel-Aziz, M. I. et al. Sputum microbiome profiles identify severe asthma phenotypes of relative stability at 12 to 18 months. *J. Allergy Clin. Immunol.* **147**, 123–134 (2021).
41. Arnold, I. C. et al. Helicobacter pylori infection prevents allergic asthma in mouse models through the induction of regulatory T cells. *J. Clin. Invest* **121**, 3088–3093 (2011).
42. Kyburz, A. et al. Transmaternal Helicobacter pylori exposure reduces allergic airway inflammation in offspring through regulatory T cells. *J. Allergy Clin. Immunol.* **143**, 1496–1512 (2019). e1411.
43. Engler, D. B. et al. Effective treatment of allergic airway inflammation with Helicobacter pylori immunomodulators requires BATF3-dependent dendritic cells and IL-10. *Proc. Natl Acad. Sci. USA* **111**, 11810–11815 (2014).
44. Barcik, W., Boutin, R. C. T., Sokolowska, M. & Finlay, B. B. The role of lung and gut microbiota in the pathology of asthma. *Immunity* **52**, 241–255 (2020).
45. Fujimura, K. E. et al. House dust exposure mediates gut microbiome Lactobacillus enrichment and airway immune defense against allergens and virus infection. *Proc. Natl Acad. Sci. USA* **111**, 805–810 (2014).
46. Wu, C.-T., Chen, P.-J., Lee, Y.-T., Ko, J.-L. & Lue, K.-H. Effects of immunomodulatory supplementation with Lactobacillus rhamnosus on airway inflammation in a mouse asthma model. *J. Microbiol. Immunol. Infect.* **49**, 625–635 (2016).
47. Louis, P. & Flint, H. J. Diversity, metabolism and microbial ecology of butyrate-producing bacteria from the human large intestine. *FEMS Microbiol. Lett.* **294**, 1–8 (2009).
48. Roduit, C. et al. High levels of butyrate and propionate in early life are associated with protection against atopy. *Allergy* **74**, 799–809 (2019).
49. Yip, W. et al. Butyrate shapes immune cell fate and function in allergic asthma. *Front. Immunol.* **12**, 628453 (2021).
50. Altobelli, A., Bauer, M., Velez, K., Cover, T. L. & Muller, A. Helicobacter pylori VacA targets myeloid cells in the gastric lamina propria to promote peripherally induced regulatory T-cell differentiation and persistent infection. *MBio* **10**, e00261–19 (2019).
51. Abrahamsson, T. et al. Low gut microbiota diversity in early infancy precedes asthma at school age. *Clin. Exp. Allergy* **44**, 842–850 (2014).
52. Cahenzli, J., Koller, Y., Wyss, M., Geuking, M. B. & McCoy, K. D. Intestinal microbial diversity during early-life colonization shapes long-term IgE levels. *Cell Host Microbe* **14**, 559–570 (2013).
53. Lynch, S. V. et al. Effects of early-life exposure to allergens and bacteria on recurrent wheeze and atopy in urban children. *J. Allergy Clin. Immunol.* **134**, 593–601.e512 (2014).
54. Turnbaugh, P. J. et al. An obesity-associated gut microbiome with increased capacity for energy harvest. *Nature* **444**, 1027–1031 (2006).
55. Ivanov, I. I. et al. Induction of intestinal Th17 cells by segmented filamentous bacteria. *Cell* **139**, 485–498 (2009).
56. Dubourg, G. et al. High-level colonisation of the human gut by Verrucomicrobia following broad-spectrum antibiotic treatment. *Int. J. Antimicrobial Agents* **41**, 149–155 (2013).
57. Derrien, M., Vaughan, E. E., Plugge, C. M. & de Vos, W. M. Akkermansia muciniphila gen. nov., sp. nov., a human intestinal mucin-degrading bacterium. *Int. J. Syst. Evolut. Microbiol.* **54**, 1469–1476 (2004).
58. Bisgaard, H., Jensen, S. M. & Bønnelykke, K. Interaction between asthma and lung function growth in early life. *Am. J. Respir. Crit. Care Med.* **185**, 1183–1189 (2012).
59. Stokholm, J. et al. Maturation of the gut microbiome and risk of asthma in childhood. *Nat. Commun.* **9**, 141 (2018).
60. Zheng, D., Liwinski, T. & Elinav, E. Interaction between microbiota and immunity in health and disease. *Cell Res.* **30**, 1–15 (2020).
61. Reuter, S. et al. Coincident airway exposure to low-potency allergen and cytomegalovirus sensitizes for allergic airway disease by viral activation of migratory dendritic cells. *PLoS Pathog.* **15**, e1007595 (2019).
62. McGovern, T. K., Robichaud, A., Fereydoonzad, L., Schuessler, T. F. & Martin, J. G. Evaluation of respiratory system mechanics in mice using the forced oscillation technique. *J. Vis. Exp.* **75**, e50172 (2013).
63. Walters, W. et al. Improved bacterial 16S rRNA gene (V4 and V4-5) and fungal internal transcribed spacer marker gene primers for microbial community surveys. *mSystems* **1**, e00009-15 (2016).
64. Bolyen, E. et al. Reproducible, interactive, scalable and extensible microbiome data science using QIIME 2. *Nat. Biotechnol.* **37**, 852–857 (2019).
65. Callahan, B. J. et al. DADA2: high-resolution sample inference from Illumina amplicon data. *Nat. Methods* **13**, 581–583 (2016).
66. Katoh, K. & Standley, D. M. MAFFT multiple sequence alignment software version 7: improvements in performance and usability. *Mol. Biol. Evol.* **30**, 772–780 (2013).
67. Love, M. I., Huber, W. & Anders, S. Moderated estimation of fold change and dispersion for RNA-seq data with DESeq2. *Genome Biol.* **15**, 550 (2014).
68. Wipperman, M. F. et al. Antibiotic treatment for Tuberculosis induces a profound dysbiosis of the microbiome that persists long after therapy is completed. *Sci. Rep.* **7**, 10767 (2017).
69. Davis, N. M., Proctor, D. M., Holmes, S. P., Relman, D. A. & Callahan, B. J. Simple statistical identification and removal of contaminant sequences in marker-gene and metagenomics data. *Microbiome* **6**, 226 (2018).

ACKNOWLEDGEMENTS

We thank Dr. Leopoldo Segal, Dr. Yonghua Li, Dr. Juan Lafaille, Dr. Shruti Naik, and Angela Fallegger for scientific input and support for these studies. Dr. Elitza Ivanova for technical assistance with the methacholine challenge assay. And Drs Huilin Li and Kelly Ruggles for their input on data analysis. Study designs were generated using BioRender.

AUTHOR CONTRIBUTIONS

T.C.B. was involved in all aspects of experimental design, data acquisition, analysis, and interpretation, and drafting and revising of the manuscript. M.J.B. and A.M. were involved in experimental design, analysis, interpretation, drafting and revising manuscript. M.B.P. and X.Z. were involved in experimental design, data acquisition and analysis, and manuscript revision. M.F.W. was involved in data analysis, manuscript revision. S.B.K. and C.T. were involved in experimental design, interpretation and revising manuscript. S.R., T.I., Z.G., T.M., M.D., and J.L. were involved in data acquisition, analysis, and manuscript revision.

FUNDING

T.C.B. was supported by the National Institutes of Health (TL1TR001447, T32ES007324, T32AI007180). This work was supported by NIH U01AI22285 and the Leducq and Sergei Zlinkoff foundations for M.J.B. and the Swiss National Science Foundation (BSCGIO 462 157841/1) for A.M. Flow cytometry technologies were provided by the NYU Langone Cytometry and Cell Sorting Laboratory, and 16S rRNA sequencing provided by the NYU Genome Technology Center and were supported in part by grant P30CA016087 from the National Institutes of Health/National Cancer Institute. Work in the S.B.K. lab was supported by NIH R01HL125816. C.T. was support by the German Research Foundation (DFG) (Ta 275/7-1); S.R. was supported by the German Research Foundation (DFG) (RE 3652/4-1).

COMPETING INTERESTS

The authors declare no competing interests.

ADDITIONAL INFORMATION

Supplementary information The online version contains supplementary material available at https://doi.org/10.1038/s41385-022-00544-5.

Correspondence and requests for materials should be addressed to Anne Müller or Martin J. Blaser.

Reprints and permission information is available at http://www.nature.com/reprints

Publisher's note Springer Nature remains neutral with regard to jurisdictional claims in published maps and institutional affiliations.